A Curvature-Guided Diffeomorphic Mesh Deformation Framework for Lifespan Brain Cortical Surface Reconstruction

Lin Teng[1], Shen Zhao[2], Feng Shi[2(✉)], Dinggang Shen[1,2,3(✉)]

[1] School of Biomedical Engineering & State Key Laboratory of Advanced Medical Materials and Devices, ShanghaiTech University, Shanghai 201210, China
[2] Department of Research and Development, United Imaging Intelligence, Shanghai 200230, China
feng.shi@uii-ai.com
[3] Shanghai Clinical Research and Trial Center, Shanghai 201210, China
dgshen@shanghaitech.edu.cn

Abstract. Accurate and automatic lifespan brain cortical surface reconstruction (CSR) is crucial for analyzing brain development and aging. Traditional pipelines involve multiple processing steps, which are time-intensive and inefficient for handling larger datasets. While deep learning-based methods can accelerate reconstruction speed and produce high-quality meshes compared to traditional approaches, they are often constrained to a single time point. The limitation arises from the significant variations in cortical surfaces across age groups, particularly in folding patterns. In this paper, we propose a novel curvature-guided diffeomorphic mesh deformation framework for lifespan brain CSR. Specifically, to preserve correct topology structure and uniformity, the framework employs multiple deformation blocks to gradually warp a simple smooth template mesh to a complex target surface with high folding. Considering that curvature is closely associated with folding patterns, we introduce curvature map prediction as an auxiliary task to guide the deformation process, enhancing the anatomical accuracy to facilitate subsequent cortical morphometry. Notably, incorporating curvature can also expedite model convergence. Our method is evaluated on a large-scale brain dataset with **2,132** subjects spanning ages 0 to 100 years. Experimental results show that our reconstructed surfaces have fewer geometric errors and optimal mesh regularity while being several orders of magnitude faster than traditional pipelines. Our code is available at https://github.com/TL9792/CCF.

Keywords: Lifespan · 3D cortical surface reconstruction · Curvature-guided diffeomorphic mesh deformation · Deep learning.

1 Introduction

The human brain undergoes dramatic changes in size, shape, and tissue intensity distribution throughout the lifespan[1], particularly during the first postnatal

[1] **Lifespan** refers to the duration of an organism's life, from birth to old age.

year [1]. These changes are especially prominent in cortical surfaces[2], where cortical shape and thickness vary with age. Compared to volumetric data, the cortical surface provides more detailed geometric representations of the brain, enabling the visualization of cortical structures and supporting various downstream analyses by calculating cortical properties (*e.g.*, cortical curvature and thickness) [23]. Consequently, accurate brain cortical surface reconstruction (CSR) from volumetric data is crucial for understanding brain development, aging, and associated neurodegenerative disease diagnosis.

Traditional surface analysis packages designed for a single time point, such as Infant FreeSurfer [24], FreeSurfer [8], and FastSurfer [10], typically involve multiple time-consuming steps. This makes it challenging to efficiently analyze large datasets. To address this, deep learning-based CSR approaches have emerged, and these can be broadly categorized into implicit and explicit methods depending on the 3D shape representation they operate on. Implicit methods leverage deep neural network (DNN) to learn an implicit surface representation, such as an occupancy field and a signed distance function (SDF) [4, 7, 8, 10, 16]. For example, Cruz *et al.* [4] proposed DeepCSR, a model that predicts implicit surface representations for points and subsequently applies an isosurface extraction method to reconstruct adult brain cortical surfaces. However, these implicit methods often fail to ensure the quality of reconstructed meshes with topology correctness. For explicit methods [13, 14, 18, 22], a DNN is trained in an end-to-end manner to directly generate an explicit mesh by deforming an initial mesh into a target mesh. For example, Ma *et al.* [14] proposed a PialNN to generate outer surfaces from inner surfaces as input through multiple deformation blocks. Similarly, Lebrat *et al.* [18] proposed CorticalFlow^{++}, which employs diffeomorphic mesh deformation (DMD) modules to learn a series of stationary velocity fields (SVF) defining diffeomorphic deformations from an initial template to inner and outer surfaces. These explicit methods have gained attention for their capability to preserve topological accuracy while achieving exceptional computational efficiency. However, they often ignore the deformation of key regions with high folding, making it challenging to reconstruct brain cortical surfaces with significant variations across large-scale age groups.

Here, we propose a curvature-guided diffeomorphic mesh deformation framework for lifespan brain CSR. Specifically, we build upon CorticalFlow^{++} as our baseline due to its efficiency in preserving topology details. Beyond CorticalFlow^{++}, we use brain tissue segmentation maps predicted from our proposed segmentation model [19, 20] rather than brain MR images as input. This allows the model to focus directly on interfaces between different tissues, thereby alleviating the partial volume effect (PVE) problem commonly encountered in brain MR images. Moreover, we introduce curvature as prior knowledge to guide the diffeomorphic deformation of high-folding regions through a multi-task learning strategy. This

[2] **Brain cortical surface** consists of inner/white and outer/pial cerebral cortex in each hemisphere. The inner surface refers to the boundary between white matter (WM) and gray matter (GM), and the outer surface is the interface between GM and cerebrospinal fluid (CSF) [5].

enhances reconstruction accuracy, particularly in regions with rich anatomical information, such as sulci and gyri. Notably, introducing curvature not only improve accuracy but also accelerate convergence without increasing GPU consumption. The proposed method is evaluated on a large-scale lifespan brain dataset, and experimental results demonstrate that our mesh outperforms other state-of-the-art (SOTA) methods in terms of geometry and regularity.

2 Methodology

Fig. 1 illustrates our proposed framework for lifespan brain CSR, which consists of a series of curvature-guided deformation blocks that are trained sequentially (detailed in Section 2.1). Each block comprises one UNet-like architecture [3] (detailed in Section 2.3) and a DMD module [13]. The UNet-like model predicts a curvature-aware flow field that estimates per-vertex displacement vectors on the current state of deformation and a curvature map. The DMD module computes a diffeomorphic mapping to transform an initial template mesh into the target mesh, such as inner or outer surfaces, shown in Section 2.2.

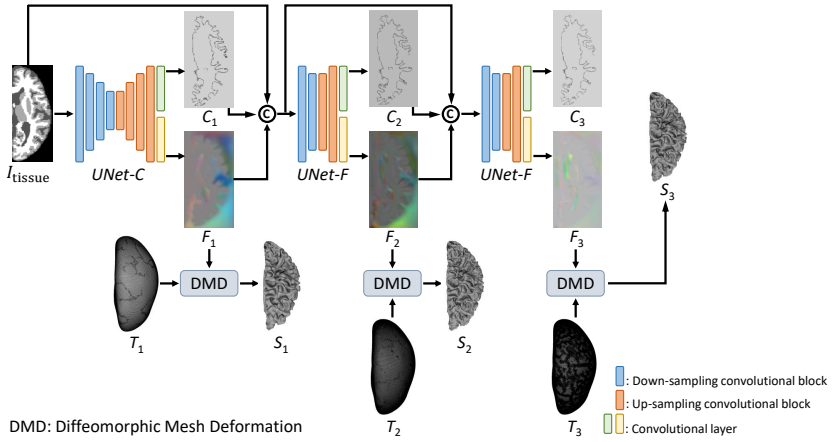

Fig. 1. An overview of our proposed curvature-guided diffeomorphic mesh deformation framework for lifespan brain CSR. The framework consists of multiple curvature-guided deformation blocks to sequentially deform an initial template mesh to the target mesh through a coarse-to-fine learning strategy (*i.e.*, inner or outer surfaces).

2.1 Overview

To mitigate the challenges associated with large deformations from a smooth template mesh to a complex brain cortical surface, we adopt a coarse-to-fine learning strategy. This approach decomposes a substantial deformation into

multiple simpler deformations, enhancing both accuracy and efficiency. The framework includes three sequential deformation stages for reconstructing inner and outer surfaces of each brain hemisphere. Specifically, in the initial stage, a 3D brain tissue segmentation map (I_{tissue}) with dimension H×W×D×1 is fed into the first deformation model (UNet-C), and the output includes a curvature-aware flow field (F_1) of dimension H×W×D×3 and a curvature map (C_1) of dimension H×W×D×1 (detailed in Section 2.2). Subsequently, F_1 and a smooth template mesh comprising 40k vertices (T_1) are processed through a DMD module to produce a coarse cortical surface (S_1). In the second stage, the concatenation of I_{tissue}, F_1, and C_1 serve as input to the second deformation model UNet-F, and the output includes a curvature-aware flow field (F_2) and curvature map (C_2). Both F_2 and T_2 with 140k vertices are fed into DMD module to yield a refined cortical surface (S_2). The third deformation stage mirrors the second, differing only in the use of a template mesh with 380k vertices (T_3). This hierarchical approach ensures a progressive refinement of the cortical surface, effectively capturing intricate anatomical details. The total deformation equation is as follows:

$$\begin{aligned} F_1, C_1 &= \text{UNet-C}(I_{tissue}), \\ S_1 &= \text{DMD}\left(F_1, \mathcal{T}_1\right), \\ F_{i+1}, C_{i+1} &= \text{UNet-F}_{i+1}\left(F_1 \frown C_1 \cdots F_i C_i I_{tissue}\right), \quad \text{for } i \geq 1. \\ S_{i+1} &= \text{DMD}\left(F_{i+1}, T_{i+1}\right), \end{aligned} \tag{1}$$

where F_i, C_i, and S_i are i-th predicted curvature-aware flow field, i-th predicted curvature map, and i-th reconstructed surface, respectively. i is the number of deformation iteration, *i.e.*, $i = 3$. $\frown$ represents the concatenation operator.

2.2 Curvature-Guided Diffeomorphic Mesh Deformation

Cortical surfaces exhibit significant variations across different age groups, particularly in detailed sulcal and gyral patterns. These variations pose challenges in accurately aligning a template with each individual's unique cortical structure while preserving the fine details of the surface topology. To solve this issue, we introduce curvature as prior knowledge to guide the deformation process. Curvature effectively quantifies the folding patterns of cortical surfaces, capturing both local variations in surface shape and the overall structure of the brain's gyral and sulcal regions.

Curvature Map Generation. Due to the lack of a one-to-one correspondence between the vertices of the template mesh and the pseudo-ground truth, we generate the curvature map within volumetric space rather than directly on the surface. Initially, we compute the mean curvature value at each vertex of the pseudo-ground-truth cortical surface using the PyVista library. To align them with brain MR image, these vertex-specific curvature values are then mapped into 3D volumetric space by correlating vertex coordinates to voxel positions.

The process yields a curvature map as C with dimension of H×W×D, where H, W, and D are the length, width, and depth of brain MR image, respectively. Finally, the curvature values are normalized to a range between -1 and 1, where negative values represent sulcal regions while positive values are gyral regions.

Multi-Task Learning. To effectively utilize curvature to guide the deformation of critical regions, we adopt a multi-task learning strategy. Each deformation model is designed with two branches: one for predicting a curvature-aware flow field and the other for predicting a curvature map. By using curvature map prediction as an auxiliary task, the model becomes more anatomy-aware, enabling it to better capture features in high-folded regions. This approach enhances the model's ability to reconstruct cortical surfaces with high accuracy, particularly in regions with complex anatomical structures.

Curvature-aware Diffeomorphic Deformation. To accurately deform a template mesh to the target mesh, the predicted curvature-aware flow field (F) and a template mesh (T) are fed into a DMD module, computing a diffeomorphic mapping ϕ as an ordinary differential equation (ODE) for each vertex position $x \in \mathbb{R}^3$, to obtain a new mesh that is closer to the target mesh. Formally, the procedure of solving the flow ODE

$$\frac{\partial \phi_i\left(s; x_{i,k}\right)}{\partial s} = U_i\left(\phi_i\left(s; x_{i,k}\right)\right), \phi_i\left(0; x_{i,k}\right) = x_{i-1,k}, \tag{2}$$

using the fourth-order Runge-Kutta (RK4) with 30 time-steps [17]. ϕ_i, U_i, and $x_{i,k}$ are the i-th diffeomorphic mapping, the i-th curvature-aware flow field, and the k-th vertex of i-th surface, respectively. The condition is that $x_{i,k}$ is the same as $x_{i-1,k}$ when s=0. Formulating a deformation as an ODE significantly reduces the occurrence of self-intersecting faces, thereby more accurately approximating the target surface.

2.3 Network Architecture

The framework comprises three sub-networks with a 3D UNet-shape architecture: UNet-C and two UNet-F. UNet-C consists of four down-/up-sampling convolutional blocks and two 3×3×3 convolutional layers, and UNet-F has two down/up-sampling convolutional blocks and two convolutional layers. Down-sampling convolutional block includes a 3×3×3 convolutional layer and a LeakyReLU activation layer. Up-sampling convolutional block includes a 3×3×3 convolutional layer, a LeakyReLU activation layer, and a transposed convolutional layer. The rationale behind this architectural change is to facilitate the learning of coarse-to-fine deformations [13].

2.4 Loss Function

The training process is supervised by a composite loss function comprising Chamfer distance loss L_{cd} [22], edge length loss L_{edge} [22], and curvature loss

$L_{curvature}$, each weighted by hyperparameters λ_1, λ_2, and λ_3, respectively.

$$L(S_p, S_g, C_p, C_g) = \lambda_1 L_{cd}(S_p, S_g) + \lambda_2 L_{edge}(S_p) + \lambda_3 L_{curvature}(C_p, C_g), \quad (3)$$

where L_{cd} and L_{edge} are computed on 150k points from uniformly sampling at random on the predicted (S_p) and pseudo-ground-truth surfaces (S_g). $L_{curvature}$ calculates the mean absolute error between the predicted (C_p) and ground truth curvature map (C_g). λ_1, λ_2, and λ_3 are set to 1.0, 1.0, and 0.001 based on the magnitude of loss values, respectively.

3 Experiments and Results

3.1 Datasets and Metrics

We have compiled a comprehensive lifespan brain dataset encompassing individuals aged 0 to 100 years, comprising **2,132** T1-weighted (T1w) MR images sourced from 18 repositories. These include 341 subjects (0-6 years) from Baby Connectome Project (BCP) [11], 30 subjects (9-11 years) from Adolescent Brain Cognitive Development (ABCD) [2], 295 subjects (18-81 years) from CBMFM [9], 22 subjects (18-94 years) from Open Access Series of Imaging Studies (OASIS) [15], 129 subjects (56-96 years) from Alzheimer's Disease Neuroimaging Initiative (ADNI) [12], 69 subjects (6-56 years) from Autism Brain Imaging Data Exchange (ABIDE) [6], and 875 subjects (2-95 years) from private hospitals. Each subject has a T1w MR image, a tissue segmentation map generated by our previously developed segmentation model mentioned above, and pseudo-ground-truth surfaces derived using Infant FreeSurfer [24] and FreeSurfer pipelines with different smoothing parameters set, based on our tissue segmentation maps. The T1w MR image is preprocessed with skull stripping, intensity normalization, and bias field correction [21]. All volume data are standardized to a resolution of 193×229×193 with voxel spacing of 1.0×1.0×1.0 mm^3. Each dataset is randomly partitioned into training, validation, and testing in a ratio of 8:1:1 for each age group [1]. Performance is evaluated using Chamfer distance (CD), 95th-percentile Hausdorff distance (HD), and normal consistency (NC) calculated for point clouds of 200k points with uniform sampling.

3.2 Implementation Details

Experiments are implemented on one NVIDIA A100 GPU with 40GB memory. Each deformation model is trained with 70K iterations for inner surface reconstruction. After that, the estimated inner surfaces serve as the initial template mesh to reconstruct outer surfaces, in which each deformation model is trained with 70K iterations while freezing the parameters of the white model. This ensures a one-to-one mapping between the vertices of the inner and outer surfaces, facilitating brain analysis. An Adam optimizer with an initial learning rate of e^{-4} is used. Batch size is 3.

Table 1. Quantitative comparison of brain cortical surfaces from different SOTA methods in terms of CD, HD, and NC (↑ and ↓ denote larger and smaller values, respectively. \ is no result. The best results are in **bold**).

Method	Left Inner Surface			Right Inner Surface		
	CD (mm) ↓	HD (mm) ↓	NC ↑	CD (mm) ↓	HD (mm) ↓	NC ↑
PialNN	\	\	\	\	\	\
DeepCSR	4.98±21.49	1.71±2.80	0.88±0.06	3.00±10.77	1.45±1.98	0.89±0.06
CorticalFlow^{++}	1.31±1.22	1.15±0.47	0.88±0.06	1.02±0.93	1.01±0.39	0.89±0.05
Ours	**0.46±0.22**	**0.69±0.10**	**0.95±0.01**	**0.53±0.18**	**0.76±0.10**	**0.94±0.01**
	Left Outer Surface			Right Outer Surface		
	CD (mm) ↓	HD (mm) ↓	NC ↑	CD (mm) ↓	HD (mm) ↓	NC ↑
PialNN	1.36±0.54	1.27±0.29	0.87±0.02	1.26±0.44	1.21±0.24	0.87±0.02
DeepCSR	4.91±4.19	3.00±1.44	0.84±0.04	5.37±4.56	3.18±1.41	0.84±0.04
CorticalFlow^{++}	1.25±1.44	1.06±0.56	0.87±0.05	1.10±1.16	1.04±0.52	0.91±0.04
Ours	**0.47±0.18**	**0.68±0.09**	**0.94±0.01**	**0.51±0.09**	**0.77±0.06**	**0.95±0.01**

3.3 Results

Comparison with SOTA methods. We evaluated our method against several representative SOTA methods in brain CSR, including PialNN, DeepCSR, and CorticalFlow^{++}. To ensure a fair comparison, we reproduced all methods using their official code and applied the same dataset and partition strategy.

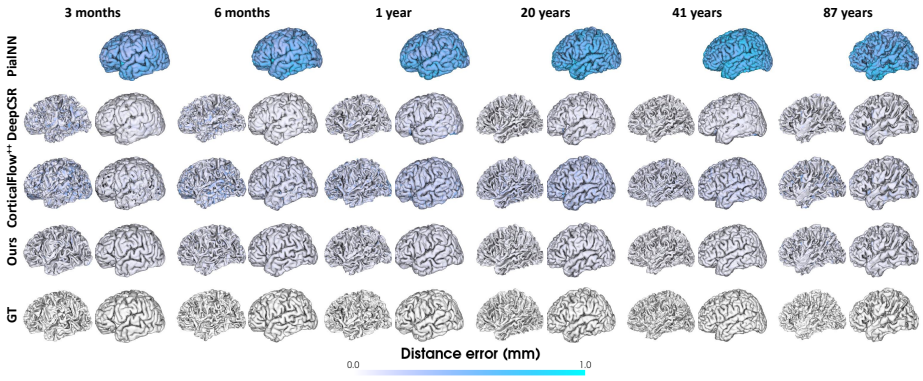

Fig. 2. Reconstructed left inner and outer surfaces across different age groups from different SOTA methods, which are color-coded with distance errors relative to pseudo-ground-truth surfaces.

Table 1 shows the quantitative comparison of brain CSR from different SOTA methods in terms of CD, HD, and NC. As we can see, our method outperforms other SOTA methods on all metrics. For example, PialNN shows relatively strong performance in outer surface reconstruction, although it is not suitable

for reconstructing inner surfaces. DeepCSR exhibits the poorest performance in all metrics, likely due to its implicit representation learning approach that does not ensure topological correctness. In contrast, our method achieves significant improvements over the baseline (*i.e.*, CorticalFlow^{++}), with reductions of 0.78 mm in CD, 0.38 mm in HD, and 0.11 in NC for left outer surface reconstruction, respectively. Fig. 2 visualizes predicted left cortical surfaces across multiple age groups, color-coded to indicate the distance to pseudo-ground-truth surfaces from different SOTA methods. Our surfaces have smaller geometric errors than other SOTA methods, as evidenced by the distance errors overlaid on the surfaces. For example, reconstructed surfaces from CorticalFlow^{++} exhibit significant errors in highly folded regions (*e.g.*, sulci and gyri). Besides, our method is more robust than other methods. Compared to DeepCSR and PialNN, our reconstructed surfaces across multiple age groups are more consistent.

Ablation Study. We conduct an ablation study to assess the impact of using the tissue segmentation map as input and adding the curvature prediction branch on the performance of lifespan brain CSR.

Tissue Segmentation Map as Input We conduct two experiments based on CorticalFlow^{++} using either brain MR image or tissue segmentation map as input to verify the benefit of incorporating tissue-specific information, respectively. Experimental results show that CorticalFlow^{++}+I$_{tissue}$ achieves CD, HD, and NC of 0.63/0.67 mm, 0.83/0.85 mm, and 0.90/0.90 for left inner/outer surface reconstruction, and 0.72/0.73 mm, 0.86/0.86 mm, and 0.91/0.93 for right inner/outer surface reconstruction, respectively. Compared to CorticalFlow^{++}, CorticalFlow^{++}+I$_{tissue}$ brings improvements of 68% in CD and 32% in HD for left inner surface reconstruction. This demonstrates that tissue maps provide clearer boundary information, effectively mitigating the PVE effects present in brain MR images.

Curvature Prediction Branch Building upon CorticalFlow^{++}+I$_{tissue}$, we introduce a curvature prediction branch using a multi-task learning strategy. Compared to CorticalFlow^{++}+I$_{tissue}$, curvature prior brings improvements across all metrics, including 18%/21% (CD) and 12%/13% (HD) for inner/outer surface reconstruction. This highlights that curvature prediction provides additional anatomical features for deformation models, leading to enhanced reconstruction accuracy and structural fidelity. Furthermore, incorporating curvature reduces the convergence time from 3.5 days to 3 days.

4 Conclusion

In this paper, we have presented a novel curvature-guided flow-based approach for efficient lifespan brain CSR. To preserve accurate topology and anatomical properties for cortical surfaces with large variations across multiple age groups, the framework consists of several curvature-guided deformation blocks that gradually

transform a smooth template mesh to the inner surface and subsequently into the outer surface using a coarse-to-fine strategy. Experiments conducted on extensive lifespan brain datasets demonstrate that our method achieves more precise mesh regularity and better preservation of cortical folding patterns compared to other SOTA methods. Therefore, this method will be integrated into our developed lifespan brain analysis pipeline to support clinical studies of brain development and aging.

Acknowledgments. This work was supported in part by National Natural Science Foundation of China (82441023, U23A20295, 62131015, 82394432), National Key Technologies R&D Program of China (82027808), the China Ministry of Science and Technology (S20240085, STI2030-Major Projects-2022ZD0209000, STI2030-Major Projects-2022ZD0213100), Shanghai Municipal Central Guided Local Science and Technology Development Fund (No. YDZX20233100001001), The Key R&D Program of Guangdong Province, China (2023B0303040001), and HPC Platform of ShanghaiTech University.

Disclosure of Interests. S.Z., F.S., and D.S. are employees of United Imaging Intelligence. The company has no role in designing and performing the surveillances and analyzing and interpreting the data. All other authors report no conflicts of interest relevant to this article.

References

1. Bethlehem, R.A., Seidlitz, J., White, S.R., Vogel, J.W., Anderson, K.M., Adamson, C., Adler, S., Alexopoulos, G.S., Anagnostou, E., Areces-Gonzalez, A., et al.: Brain charts for the human lifespan. Nature **604**(7906), 525–533 (2022)
2. Casey, B.J., Cannonier, T., Conley, M.I., Cohen, A.O., Barch, D.M., Heitzeg, M.M., Soules, M.E., Teslovich, T., Dellarco, D.V., Garavan, H., et al.: The adolescent brain cognitive development (abcd) study: imaging acquisition across 21 sites. Developmental cognitive neuroscience **32**, 43–54 (2018)
3. Çiçek, Ö., Abdulkadir, A., Lienkamp, S.S., Brox, T., Ronneberger, O.: 3d u-net: learning dense volumetric segmentation from sparse annotation. In: Medical Image Computing and Computer-Assisted Intervention–MICCAI 2016: 19th International Conference, Athens, Greece, October 17-21, 2016, Proceedings, Part II 19. pp. 424–432. Springer (2016)
4. Cruz, R.S., Lebrat, L., Bourgeat, P., Fookes, C., Fripp, J., Salvado, O.: Deepcsr: A 3d deep learning approach for cortical surface reconstruction. In: Proceedings of the IEEE/CVF Winter Conference on Applications of Computer Vision. pp. 806–815 (2021)
5. Dale, A.M., Fischl, B., Sereno, M.I.: Cortical surface-based analysis: I. segmentation and surface reconstruction. Neuroimage **9**(2), 179–194 (1999)
6. Di Martino, A., Yan, C.G., Li, Q., Denio, E., Castellanos, F.X., Alaerts, K., Anderson, J.S., Assaf, M., Bookheimer, S.Y., Dapretto, M., et al.: The autism brain imaging data exchange: towards a large-scale evaluation of the intrinsic brain architecture in autism. Molecular psychiatry **19**(6), 659–667 (2014)

7. Fan, J., Cao, X., Wang, Q., Yap, P.T., Shen, D.: Adversarial learning for mono-or multi-modal registration. Medical image analysis **58**, 101545 (2019)
8. Fischl, B.: Freesurfer. Neuroimage **62**(2), 774–781 (2012)
9. Gu, D., Shi, F., Hua, R., Wei, Y., Li, Y., Zhu, J., Zhang, W., Zhang, H., Yang, Q., Huang, P., Jiang, Y., Bo, B., Li, Y., Zhang, Y., Zhang, M., Wu, J., Shi, H., Liu, S., He, Q., Zhang, Q., Zhang, X., Wei, H., Liu, G., Xue, Z., Shen, D., of Chinese Brain Molecular, C., (CBMFM), F.M.: An artificial-intelligence-based age-specific template construction framework for brain structural analysis using magnetic resonance images. Human Brain Mapping **44**(3), 861–875 (Feb 2023)
10. Henschel, L., Conjeti, S., Estrada, S., Diers, K., Reuter, M.: Fastsurfer - a fast and accurate deep learning based neuroimaging pipeline. NeuroImage **219**, 117012 (2020)
11. Howell, B.R., Styner, M.A., Gao, W., Yap, P.T., Wang, L., Baluyot, K., Yacoub, E., Chen, G., Potts, T., Salzwedel, A., et al.: The unc/umn baby connectome project (bcp): An overview of the study design and protocol development. NeuroImage **185**, 891–905 (2019)
12. Jack Jr, C.R., Bernstein, M.A., Fox, N.C., Thompson, P., Alexander, G., Harvey, D., Borowski, B., Britson, P.J., L. Whitwell, J., Ward, C., et al.: The alzheimer's disease neuroimaging initiative (adni): Mri methods. Journal of Magnetic Resonance Imaging: An Official Journal of the International Society for Magnetic Resonance in Medicine **27**(4), 685–691 (2008)
13. Lebrat, L., Santa Cruz, R., de Gournay, F., Fu, D., Bourgeat, P., Fripp, J., Fookes, C., Salvado, O.: Corticalflow: a diffeomorphic mesh transformer network for cortical surface reconstruction. Advances in Neural Information Processing Systems **34**, 29491–29505 (2021)
14. Ma, Q., Robinson, E.C., Kainz, B., Rueckert, D., Alansary, A.: Pialnn: a fast deep learning framework for cortical pial surface reconstruction. In: Machine Learning in Clinical Neuroimaging: 4th International Workshop, MLCN 2021, Held in Conjunction with MICCAI 2021, Strasbourg, France, September 27, 2021, Proceedings 4. pp. 73–81. Springer (2021)
15. Marcus, D.S., Wang, T.H., Parker, J., Csernansky, J.G., Morris, J.C., Buckner, R.L.: Open access series of imaging studies (oasis): cross-sectional mri data in young, middle aged, nondemented, and demented older adults. Journal of cognitive neuroscience **19**(9), 1498–1507 (2007)
16. Park, J.J., Florence, P., Straub, J., Newcombe, R., Lovegrove, S.: Deepsdf: Learning continuous signed distance functions for shape representation. In: Proceedings of the IEEE/CVF conference on computer vision and pattern recognition. pp. 165–174 (2019)
17. Press, W., Flannery, B., Teukolsky, S., Vetterling, W.: Runge-kutta method in numerical recipes in fortran: The art of scientific computing (1992)
18. Santa Cruz, R., Lebrat, L., Fu, D., Bourgeat, P., Fripp, J., Fookes, C., Salvado, O.: Corticalflow++: Boosting cortical surface reconstruction accuracy, regularity, and interoperability. In: International Conference on Medical Image Computing and Computer-Assisted Intervention. pp. 496–505. Springer (2022)
19. Teng, L., He, Y., Cao, Z., Hua, R., Han, Y., Feng, Q., Shi, F., Shen, D.: Unified model for children's brain image segmentation with co-registration framework guided by longitudinal mri. IEEE Journal of Biomedical and Health Informatics (2024)
20. Teng, L., Zhao, Z., Huang, J., Cao, Z., Meng, R., Shi, F., Shen, D.: Knowledge-guided prompt learning for lifespan brain mr image segmentation. In: International

Conference on Medical Image Computing and Computer-Assisted Intervention. pp. 238–248. Springer (2024)
21. Tustison, N.J., Avants, B.B., Cook, P.A., Zheng, Y., Egan, A., Yushkevich, P.A., Gee, J.C.: N4itk: improved n3 bias correction. IEEE transactions on medical imaging **29**(6), 1310–1320 (2010)
22. Wickramasinghe, U., Remelli, E., Knott, G., Fua, P.: Voxel2mesh: 3d mesh model generation from volumetric data. In: Medical Image Computing and Computer Assisted Intervention–MICCAI 2020: 23rd International Conference, Lima, Peru, October 4–8, 2020, Proceedings, Part IV 23. pp. 299–308. Springer (2020)
23. Zhao, F., Wu, Z., Li, G.: Deep learning in cortical surface-based neuroimage analysis: a systematic review. Intelligent Medicine **3**(1), 46–58 (2023)
24. Zöllei, L., Iglesias, J.E., Ou, Y., Grant, P.E., Fischl, B.: Infant freesurfer: An automated segmentation and surface extraction pipeline for t1-weighted neuroimaging data of infants 0–2 years. Neuroimage **218**, 116946 (2020)